Eur. Phys. J. C 10, 265–270 (1999)
Digital Object Identifier (DOI) 10.1007/s100529900108

THE EUROPEAN PHYSICAL JOURNAL C

A-dependences of neutral strange particle yields in $\bar{p}$-nuclei collisions at 40 GeV/c

T. Grigalashvili, L. Chikovani, E. Ioramashvili, A. Javrishvili, L. Khizanishvili, E. Mailian, M. Nickoladze, L. Shalamberidze

Institute of Physics, Georgian Academy of Sciences, Tamarashvili st. 6, Tbilisi, 380077 Georgia
(etheri@iph.hepi.edu.ge, eior@physics.iberiapac.ge)

Received: 10 October 1998 / Revised version: 1 April 1999 / Published online: 12 August 1999

Abstract. The interactions of $\bar{p}$ with ^{2}D, ^{7}Li, ^{12}C, ^{32}S, ^{64}Cu and ^{207}Pb nuclei at 40 GeV/c were studied by the RISC-streamer chamber spectrometer. The yields of K^0 mesons and Λ and $\bar{\Lambda}$ hyperons as functions of the target nucleus mass number are investigated. The experimental results are compared with model predictions using the FRITIOF-7.02 program package.

1 Introduction

Investigation of strange hadron production in $\bar{p}p$ and $\bar{p}A$ interactions is of a great interest because of several reasons. Firstly, as in any other hadron–hadron collisions, particles with nonzero strangeness can be produced involving sea $s\bar{s}$ quarks in the hadronization process. The study of such a production process gives information on $s\bar{s}$ pair formation and on their hadronization mechanism.

Secondly, the availability of data on strange particle production in different reactions permits one to carry out a comparative analysis of the production of nonzero strangeness hadrons. An excess of strange mesons and baryons in $\bar{p}p$ collisions in comparison with pp interactions at 32 GeV/c was observed [1–3]. Further study of neutral strange particle production gave evidence of the equivalence of pp and nonannihilation $\bar{p}p$ interactions [4].

It was shown [3,5] that at 32 GeV/c the main excess in the strange particle production cross section at $\bar{p}p$ interactions is connected with the $\bar{p}p$ annihilation process.

The meson multiplicity increases with the energy in $\bar{p}p$ annihilation processes, as in other hadron interactions [6] (and the valence quarks and antiquarks of initial nucleons can be a part of different secondary mesons). For the production of $s\bar{s}$ pairs in $\bar{p}p$ annihilation a larger fraction of the total energy can be spent as compared to pp interactions. This is caused by the fact that in pp interactions part of the total energy ($\sim 50\%$ at our energy) is consumed by leading quark spectators which, according to present knowledge, have a week influence on the process of the formation of secondary hadrons [7].

However, in $\bar{p}p$ annihilation all initial quarks and antiquarks can participate in the formation of the $s\bar{s}$ pair. In quark parton models based on QCD such a mechanism of particle production in $\bar{p}p$ interactions is realized by annihilation, e.g. by connecting more than one valence $q\bar{q}$ pairs. In quark models based on the dual topological unitarization scheme $\bar{p}p$ annihilation is described by "three-chain" diagram [8] in which all three $q\bar{q}$ pairs participate in the creation of $s\bar{s}$ pairs.

The present article deals with the experimental study of the K^0, Λ and $\bar{\Lambda}$ production process in $\bar{p}A$ (D, Li, C, S, Cu, Pb) interactions at 40 GeV/c. The experimental material was obtained with the relativistic ionization streamer chamber (RISC) with a magnetic field. The RISC setup ensured 4π angular coverage.

The experimental results will be compared with model predictions using the FRITIOF-7.02 program package [9].

2 Experimental apparatus

The main part of the RISC spectrometer is a large three-gap streamer chamber ($4.7\times0.9\times0.8$) m^3 [10] placed inside a magnetic field of about 1.5 T. The HV-pulses of $\pm$400 kV and $\sim$ 20 ns duration were produced and shaped by a bipolar Marx generator and Blumlein line [11]. The chamber was filled with a helium–neon gas mixture (50% Ne; 50% He) at atmospheric pressure. The memory time of 1–2 μs was achieved by a slight admixture of SF_6. The sensitive volume of the chamber was viewed by 8 objectives, each equipped with a two-stage image intensifier [12]. In addition, the triggered events could be directly controlled by means of a television monitor.

The experiment was performed at the Serpukhov proton synchrotron, using an unseparated beam of negatively charged particles with a momentum of 40 GeV/c. The beam was composed of π^- and K^- and $\bar{p}$ in the ratio of 100 : 1.8 : 0.3 and had a momentum spread of $\Delta P/P \sim 1.5\%$.

The nuclear targets were placed in the sensitive volume of the chamber along the beam line with a spacing of

30 cm. The total thickness of all targets corresponded approximately to 12% of the proton absorption length. The elliptic target disks were mounted inside cylindrical mylar boxes filled with freon in order to avoid electrical sparks.

A telescope consisting of two scintillation counters located behind the magnet of the spectrometer served as a detector designed to select the inelastic interactions of the beam particles in the target and vetoed non-interacting beam particles. The detector excluded the events with negatively charged secondaries for which the square of the transferred four-momentum $t \leq 0.05\mathrm{GeV}/c^2$. At the same time a large part of the elastic events was excluded while the losses of inelastic events were about 3% according to the evaluation based on the experimental data [13]. A more detailed description of the detector can be found in [14].

3 Data analysis

About 18,000 frames of photographic film were scanned and 7489 inelastic $\bar{p}$ interactions with deuterium, lithium, carbon, sulphur, copper and lead nuclei were found. At the scanning stage all secondary two-prong stars V^0 (further referred to as 'vees') were selected. They are the candidates for the decays of neutral strange particles emitted from the primary vertex. A double scan of the film ensured $\sim 99\%$ efficiency in detecting the vees.

All tracks comming from the primary vertex as well as the vee itself were first measured and then geometrically reconstructed in the chamber volume. The events were retained for further analysis if: (a) the momentum error of the V^0- decay tracks is less than 10% and the residual (in space) does not exceed 1.8 mm; (b) the primary vertex is reconstructed within the target; (c) the V^0's decay inside the fiducial volume: the target dependent minimum V^0 path length and a maximum downstream length of 1 m were imposed, and the radius of the fiducial volume was chosen to ensure a minimum track length of 15 cm; (d) the space point reconstruction resolutions in the horizontal directions are $\Delta X \leq 0.1$ cm, $\Delta Y \leq 0.1$ cm, and in the vertical direction $\Delta Z \leq 0.4$ cm.

If the noncoplanarity angle between the momentum of the parent neutral particle and the directions of the V^0 decay tracks was more than 6°, the vee was rejected. (The mean uncertainty in the noncoplanarity angle is $\sim 0.7°$.) Vees rejected by this criterion are mostly due to two-prong inelastic interactions or three-body decays of neutral particles.

A vee passing the above coplanarity selection was then kinematically fitted to each of four hypotheses (K^0_S, Λ, $\bar{\Lambda}$, γ) by the method of least squares for three degrees of freedom (3DF-fit). To resolve the V^0/γ ambiguity, photon conversions were rejected by demanding $M(e^+e^-) > 30\,\mathrm{MeV}/c^2$. This cut is sufficient to reject almost all γ's and the losses of V^0's are negligible. To provide a more reliable kinematical identification we retained only vees that satisfied the following criteria: (a) for each track of a vee, the space residual was further restricted not to exceed

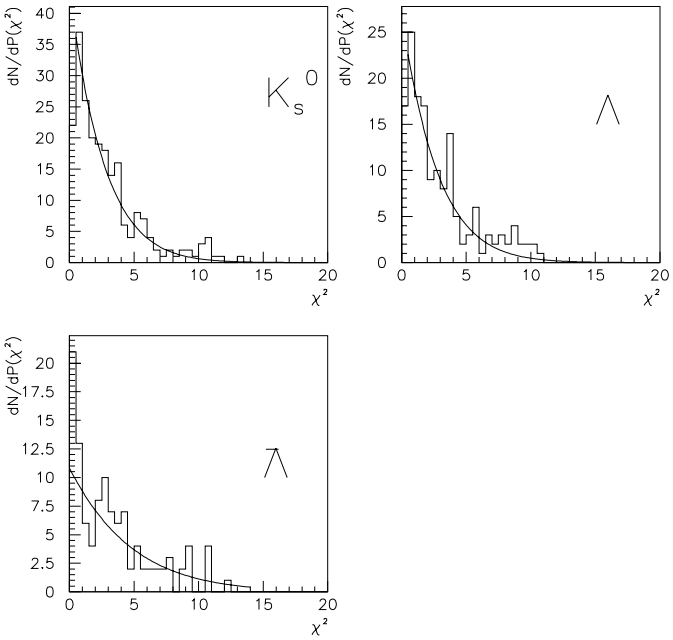

Fig. 1. Distribution of $P(\chi^2)$ for unambiguously identified particles

1.5 mm; (b) for each track of a vee, the relative momentum error $\Delta P/P \sim$ should be less than 10%.

A vee was considered as unambiguously identified if only one of the four hypotheses had a χ^2 value below 12 (see Fig. 1). The mean values of χ^2 for identified particles were

$$\langle\chi^2\rangle_{K^0_S} = 2.8 \pm 0.2, \quad \langle\chi^2\rangle_{\Lambda} = 3.0 \pm 0.2,$$
$$\langle\chi^2\rangle_{\bar{\Lambda}} = 3.3 \pm 0.3\ .$$

A vee was considered ambiguously identified if the condition $\chi^2 \leq 12$ was satisfied for two of the hypotheses. The ambiguity between Λ and K^0_S was resolved in favor of K^0_S, when the transverse momentum of the negatively charged particle from the vee exceeded 105 MeV/c within the error. The observed ionization along both tracks of a vee was also used to identify the parent V^0 (by p, $\bar{p}$, π meson identification). In total, nearly 5% of all detected neutral strange particles could not be unambiguously identified. These V^0 particles were taken into account in calculations of the yields but they did not participate in the distribution of other kinematic characteristics.

These distributions for unambiguously identified neutral strange particles are demonstrated in Figs. 2 and 3. The $\cos(\Theta^*)$ distributions for the identified strange particles are shown in Fig. 2, where Θ^* is the angle between the directions of the V^0 and one of the decay products calculated in the V^0 rest frame. The masses of K^0_S, Λ and $\bar{\Lambda}$ candidates are plotted in Fig. 3. The mean values are $\langle M_{K^0_S}\rangle = (0.490{\pm}0.003)$ GeV, $\langle M_{\Lambda}\rangle = (1.115{\pm}0.001)$ GeV and $\langle M_{\bar{\Lambda}}\rangle = (1.116 \pm 0.001)$ GeV. The correlation between the Podolansky–Armenteros parameter α and the negative decay product transverse momentum with respect to the vee direction is illustrated in Fig. 4. The bands populated by neutral strange particles of each type are clearly seen.

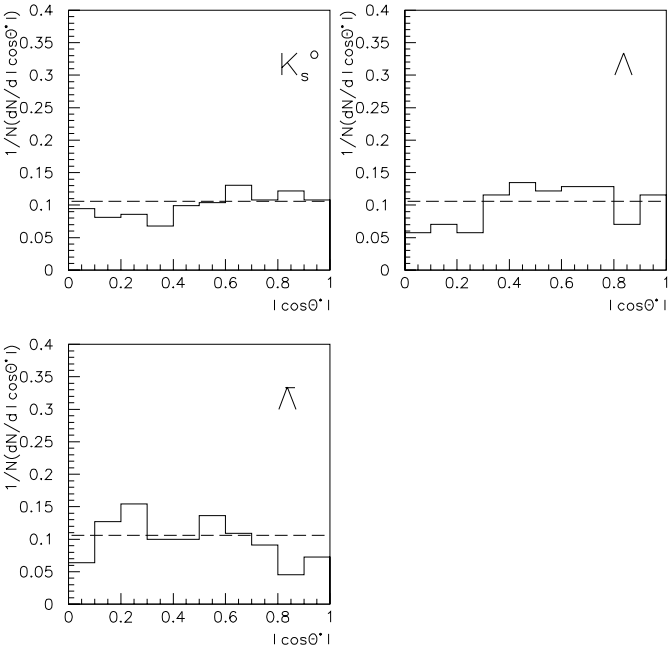

Fig. 2. Distribution of $\cos(\Theta^*)$ for unambiguously identified particles

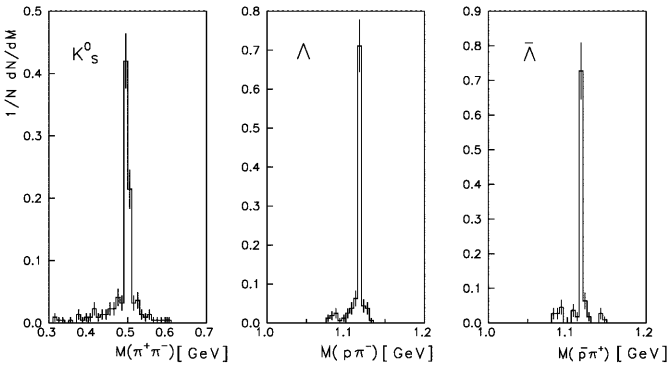

Fig. 3. Distribution of invariant mass for identified particles (for $K^0_S \to M(\pi^+\pi^-)$, for $\Lambda \to M(p\pi^-)$ and for $\bar{\Lambda} \to M(\bar{p}\pi^+)$)

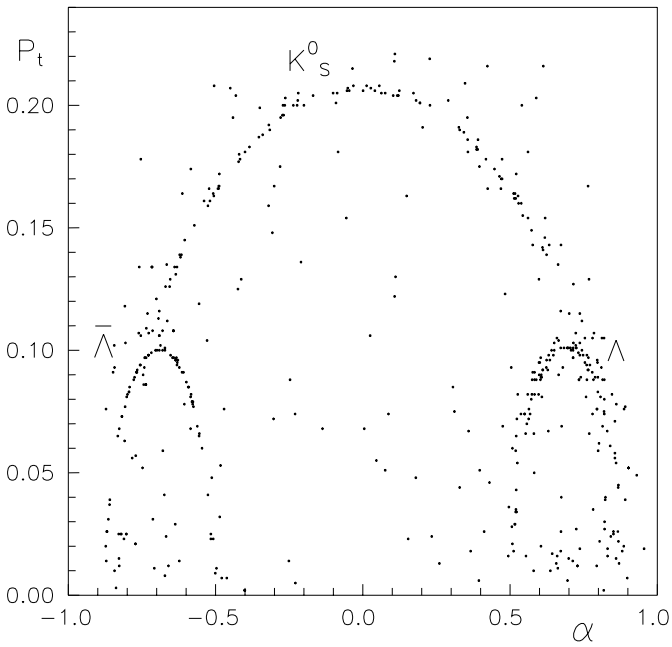

Fig. 4. Scatter plot of transverse momentum (p_t) of negative particles as a result of decays of K^0_S and Λ and $\bar{\Lambda}$ versus Podolansky–Armenteros parameter (α)

Table 1. Sum of experimental statistics and geometric correction factors

A	$N_{\rm int}$	$N_{K^0_S}$	N_Λ	$N_{\bar{\Lambda}}$	$\langle W_1\rangle_{K^0_S}$	$\langle W_1\rangle_\Lambda$	$\langle W_1\rangle_{\bar{\Lambda}}$
D	1741	35	23	27	3.6±.4	3.5±.5	2.9±.3
Li	1149	36	22	20	2.4±.3	2.2±.4	2.0±.3
C	1053	30	16	16	2.8±.4	3.2±.4	2.0±.2
S	1197	47	36	24	2.6±.2	2.4±.2	2.3±.2
Cu	1346	42	34	14	3.6±.5	3.4±.4	2.8±.4
Pb	1003	29	28	17	3.8±.6	3.6±.4	2.1±.4

To reconstruct the numbers of genuinely produced K^0 mesons, Λ hyperons and $\bar{\Lambda}$ hyperons, we introduced the required correction factors.

(1) The loss of events due to the limited dimensions of the chamber and the loss of particles in the target were taken into account by means of a geometric correction factor $\langle W_1\rangle$,

$$W_1 = 1/[\exp(L_1/L_0) - \exp(L_n/L_0)]\ ;$$

L_1 is the distance from the target below which the observation of the V^0 is difficult because of a large number of charged secondaries. L_n is the length of the potential path. L_0 is the mean decay length.

$\langle W_1\rangle$ depends on the target type since the mean multiplicity of the emitted particles grows with increasing mass number of the target. As a result, the efficiency of the determination of the vee vertex location deteriorates for larger mass numbers.

(2) The unobserved decay channels $K^0_S \to \pi^0\pi^0$, $\Lambda \to n + \pi^0$ and $\bar{\Lambda} \to \bar{n} + \pi^0$, as well as the emission of the long-lived K^0_L mesons, were taken into account by means of $W_2(K^0) = 2.92 \pm 0.06$ and $W_2(\Lambda) = 1.56 \pm 0.01$ factors. (From now on K^0 means the sum of the K^0 and $\bar{K^0}$ mesons.)

(3) The correction for the scanning efficiency was included by a factor $W_3 = 1.01$.

The overall correction factor W represents the product of the above mentioned three factors: $W = \langle W_1\rangle W_2 W_3$. The values of the geometric correction $\langle W_1\rangle_{K^0_S}$, $\langle W_1\rangle_\Lambda$, $\langle W_1\rangle_{\bar{\Lambda}}$ are presented in Table 1.

Table 2. Observed and predicted mean multiplicities of inclusive K^0 mesons and Λ and $\bar{\Lambda}$ hyperons

Sample	$\langle N_{K^0}\rangle$	$\langle N_\Lambda\rangle$	$\langle N_{\bar{\Lambda}}\rangle$
$\bar{p}p$[3] 32 GeV/c	0.21±.02	0.05±.01	0.06±.01
$\bar{p}p$[17] 100 GeV/c	0.30±.02	0.07±.01	0.07±.01
Prediction	0.1902	0.0633	0.0654
$\bar{p}D$	0.24±.02	0.07±.01	0.07±.01
Prediction	0.1997	0.0585	0.0628
$\bar{p}Li$	0.25±.02	0.07±.01	0.06±.01
Prediction	–	–	–
$\bar{p}C$	0.27±.02	0.08±.02	0.06±.02
Prediction	0.2567	0.0941	0.0741
$\bar{p}S$	0.35±.02	0.13±.01	0.07±.01
Prediction	0.3148	0.1118	0.0752
$\bar{p}Cu$	0.38±.02	0.15±.02	0.05±.02
Prediction	0.3385	0.1240	0.0791
$\bar{p}Pb$	0.42±.03	0.17±.02	0.06±.02
Prediction	0.4069	0.1503	0.0911

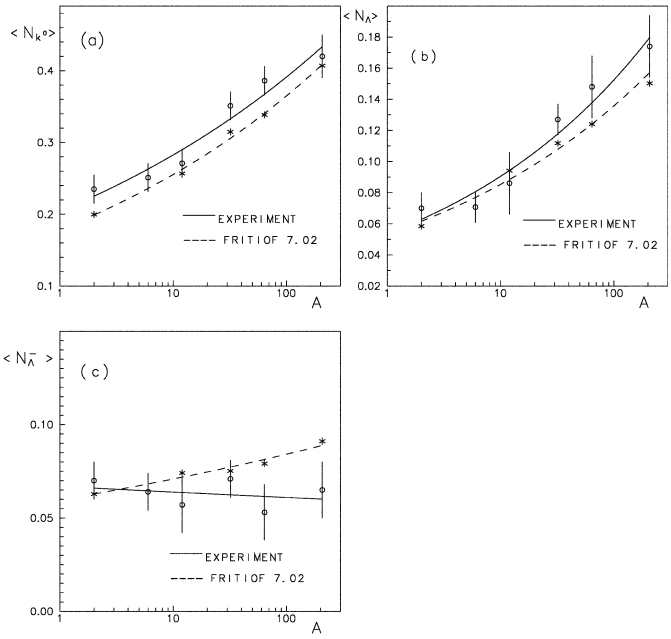

Fig. 5a–c. Mean multiplicities of **a** inclusive K^0 mesons, **b** Λ and **c** $\bar{\Lambda}$ hyperons as a function of the mass number of the target nucleus: (o) experimental data and ($*$) FRITIOF-7.02 predictions

4 Experimental results

The A-dependences of the yields of the neutral strange particles $K^0, \Lambda, \bar{\Lambda}$ were investigated in the following inclusive processes:

$$\bar{p}A \to K^0(K^0Y, K\bar{K}) + X, \quad (1)$$
$$\bar{p}A \to \Lambda(\Sigma^0) + X, \quad (2)$$
$$\bar{p}A \to \bar{\Lambda}(\bar{\Sigma}^0) + X, \quad (3)$$

where Y is short for the hyperons $\Lambda, \bar{\Lambda}, \Sigma^0, \Sigma^\pm$.

The experimental statistics used in the present article is shown in Table 1. It includes the number of inelastic interactions $N_{\rm int}$ among which V^0 events were found and the number of unambiguously identified neutral strange $K^0_S, \Lambda, \bar{\Lambda}$ particles.

After making corrections for the losses of V^0 events, as described above the total number of neutral strange particles for all studied nuclei were calculated . Thus N_Λ also includes Λ hyperons which have originated in Σ^0 decay.

On the basis of these data the average $\langle N_{K^0}\rangle$, $\langle N_\Lambda\rangle$, and $\langle N_{\bar{\Lambda}}\rangle$ multiplicities per inelastic interaction presented in Table 2 have been calculated. For comparison the values obtained by the Monte-Carlo method using the FRITIOF-7.02 program are presented for $\bar{p}A$ interactions. Table 2 also gives the average values of neutral strange particle yields obtained in $\bar{p}p$ interactions at 32 GeV/c [3] and at 100 GeV/c [15]. As is seen from Table 2 the experimental results (for K^0 and Λ) slightly exceed the model predictions. Increasing the mass number of the target nucleus from deuterium to lead the average particle multiplicities also increase: $\langle N_{K^0}\rangle$ 1.8 times, and $\langle N_\Lambda\rangle$2.5 times, but $\langle N_{\bar{\Lambda}}\rangle$ remains constant within the error. The average values of Λ and $\bar{\Lambda}$ yields are equal on a hydrogen target [3, 15], as they should due to the C-symmetry of the $\bar{p}p$ interactions.

Table 3. The parameters (a, α) and χ^2 of $y = aA^\alpha$ function for yields of neutral strange particles for experimental results and model predictions

Process	a	α	χ^2/NDF
$\bar{p}A \to K^0(K^0Y)$ + X			
Experiment	0.20±.01	0.141±.007	1.3
Prediction	0.179±0.004	0.155±0.003	
$\bar{p}$A$\to \Lambda(\Sigma^0)$ + X			
Experiment	0.054±.005	0.23±.01	0.7
Prediction	0.054±0.003	0.202±0.007	
$\bar{p}$A $\to \bar{\Lambda}(\bar{\Sigma}^0)$ + X			
Experiment	0.07±.01	−0.02±.02	0.4
Prediction	0.060±0.002	0.074±0.004	

The A-dependences of the yields of K^0 mesons and Λ and $\bar{\Lambda}$ hyperons produced in the reactions (1, 2, 3) are shown in Fig. 5a–c. The solid lines are the results of the fit to the experimental data and the dashed lines to the simulated events calculated by the FRITIOF-7.02 program with a power function $\langle N\rangle = aA^\alpha$. The parameters ($a$, α) and χ^2 are presented in Table 3.

The behavior of the yields of neutral strange particles as a function of the mass number is shown more clearly using the dependence of the relative yield $R^A_{V^0}$ (ratio of N_{K^0}, N_Λ and $N_{\bar{\Lambda}}$ for the nucleus and the corresponding values for hydrogen) and the ratio $R_{V^0} = \langle N_{K^0}\rangle/\langle N_\Lambda\rangle$

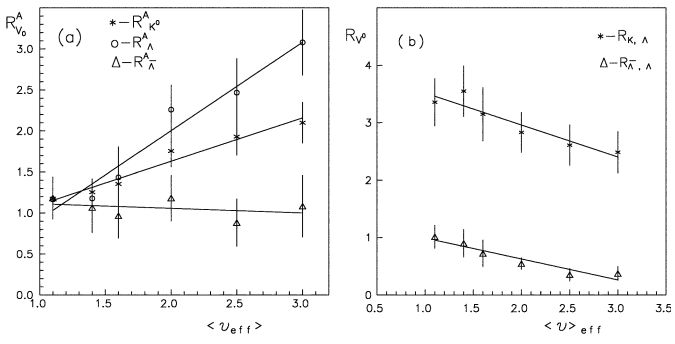

Fig. 6a and b. $R^A_{V^0}$ and R_{V^0} as functions of $\langle\nu_{\rm eff}\rangle$ (see text)

Table 4. The values of ratio of the annihilation and the inelastic cross sections $\sigma^a_{\bar{p}A}/\sigma^{inel}_{\bar{p}A}$ and corresponding $\langle\nu_{\rm eff}\rangle$ for nuclei

A	H	D	Li	C	S	Cu	Pb
$\sigma^a_{\bar{p}A}/\sigma^{inel}_{\bar{p}A}$	0.15	0.17	0.21	0.24	0.30	0.35	0.44
$\langle\nu_{\rm eff}\rangle$	1.0	1.1	1.4	1.6	2.0	2.5	3.0

Table 5. The parameters (a, b) and χ^2 of $y = a + b\langle\nu_{\rm eff}\rangle$ function for $R^A_{V^0}$ and R_{V^0} ratios for experimental results

R	a	b	χ^2/NDF
$R^A_{K^0} = \frac{\langle N_{K^0}\rangle_{\bar{p}A}}{\langle N_{K^0}\rangle_{\bar{p}p}}$	0.57 ±0.06	0.53±0.02	0.2
$R^A_{\Lambda} = \frac{\langle N_{\Lambda}\rangle_{\bar{p}A}}{\langle N_{\Lambda}\rangle_{\bar{p}p}}$	-0.155±0.004	1.07±0.05	0.5
$R^A_{\bar{\Lambda}} = \frac{\langle N_{\bar{\Lambda}}\rangle_{\bar{p}A}}{\langle N_{\bar{\Lambda}}\rangle_{\bar{p}p}}$	1.2±0.2	-0.06±0.03	0.5
$R_{K^0,\Lambda} = \frac{\langle N_{K^0}\rangle}{\langle N_{\Lambda}\rangle}$	4.1±0.8	-0.557±0.004	0.2
$R_{\bar{\Lambda},\Lambda} = \frac{\langle N_{\bar{\Lambda}}\rangle}{\langle N_{\Lambda}\rangle}$	1.4±0.2	-0.36±0.02	0.3

and $\langle N_{\bar{\Lambda}}\rangle/\langle N_{\Lambda}\rangle$ on $\langle\nu_{\rm eff}\rangle$ (Figs. 6a,b, where $\langle\nu_{\rm eff}\rangle$ is the effective number of interactions in the framework of the Glauber–Gribov model [16,17], and is determined as

$$\langle\nu_{\rm eff}\rangle = \langle\nu\rangle/\langle\nu\rangle^a$$

The vearіable $\langle\nu\rangle$, the mean number of collisions, is defined as $\langle\nu\rangle = A\sigma_{\bar{p}p}/\sigma_{\bar{p}A}$ with $\sigma_{\bar{p}p}$, $\sigma_{\bar{p}A}$ being the inelastic cross sections of $\bar{p}$ on protons and nuclei, respectively and $\langle\nu\rangle^a = A\sigma^a_{\bar{p}p}/\sigma^a_{\bar{p}A}$ is the correction for annihilation channels, where $\sigma^a_{\bar{p}p} = 5.6$ mb is taken as the difference between the sections of $\bar{p}p$ and the pp interactions at 40 GeV/c [18]. In order to estimate $\sigma^a_{\bar{p}A}$ the ratio of cross sections for the annihilation and inelastic processes $\sigma^a_{\bar{p}A}/\sigma^{inel}_{\bar{p}A}$ were calculated in the framework of the Glauber–Gribov model [19] and is given in Table 4.

All experimental results in Fig. 6a,b were fitted by linear functions, $R = a + b\langle\nu_{eff}\rangle$, the parameters of which are given in Table 5.

Thus, within the experimental error

$$R^A_{\Lambda} = (\langle N_{\Lambda}\rangle\bar{p}A)/(\langle N_{\Lambda}\rangle\bar{p}p) \approx \langle\nu_{\rm eff}\rangle$$

and

$$R^A_{\bar{\Lambda}} = (\langle N_{\bar{\Lambda}}\rangle\bar{p}A)/(\langle N_{\bar{\Lambda}}\rangle\bar{p}p) \approx 1\ .$$

A faster fall of $R_{K^0,\Lambda} = \langle N_{K^0}\rangle/\langle N_{\Lambda}\rangle$ is observed as compared to $R_{\bar{\Lambda},\Lambda} = \langle N_{\bar{\Lambda}}\rangle/\langle N_{\Lambda}\rangle$.

5 Discussion of results

The obtained results were compared with the predictions of FRITIOF-7.02 based on the quark–gluon-string model [9].

The comparison of the present experimental results with FRITIOF-7.02 calculations shows a small difference in the neutral strange particle yields. This can be explained by the fact that $\bar{p}$ annihilation is not taken into account in the model.

Therefore, the experimental value for N_{K^0} yield on heavy nuclei should be larger and the values for N_{Λ} yield should be approximately the same as the predictions since the probability of annihilation increases with increasing atomic number [19,20].

Thus the experimental results can be interpreted as follows: the differences in K^0 yields between the model and the experimental data is a consequence of the annihilation channel in $\bar{p}A$ interactions. At the same time, a part of the K^0 mesons (produced basically in the annihilation channel) can reinteract inside the nucleus. This leads to the increase of the Λ hyperon yield as the threshold energy of Λ production is small ~ 2 GeV/c [20].

The experiment shows that $\bar{\Lambda}$ hyperon yields, as was mentioned above, are practically independent on the atomic number, although the model predicts a small increase for them. Within the errors these yields are equal to those of Λ hyperons for hydrogen and deuterium.

Even when the probability of annihilation processes increases with increasing atomic number this does not give a contribution to the production of $\bar{\Lambda}$ hyperons. The K^0 mesons produced in the annihilation channel cannot create $\bar{\Lambda}$ hyperons because of the large threshold energy (~ 7 GeV [20]).

The other characteristics of the $\bar{p}A$ interactions with the production of neutral K^0 and Λ and $\bar{\Lambda}$ particles will be considered in further publications, namely the associated multiplicities of nucleons and negative mesons to the neutral strange particles; the inclusive characteristics of neutral strange particles and their dependences on the mass number of the target nuclei will be investigated.

6 Conclusion

In the present article we have investigated the production of neutral strange particles in $\bar{p}A$ collisions at 40 GeV/c in a wide range of nuclear targets (D, Li, C, S, Cu, Pb). The yields of K^0 mesons and Λ and $\bar{\Lambda}$ hyperons have been presented as a function of mass number of nuclei in the reactions $(1, 2, 3)$.

The experimental results have been compared with model predictions based on the FRITIOF-7.02 code. The following results should be mentioned:

(1) the yield of K^0 mesons in process (1) grows as

$$\sim (0.20 \pm 0.01) A^{(0.141 \pm 0.007)} .$$

(2) The yield of Λ hyperons in process (2) grows as

$$\sim (0.054 \pm 0.005) A^{(0.22 \pm 0.01)} .$$

(3) The yield of $\bar{\Lambda}$ hyperons in process (3) remains constant within the experimental errors

$$\sim (0.07 \pm 0.01) A^{(-0.02 \pm 0.02)} .$$

Thus the relative yields $R^A_\Lambda = (\langle N_\Lambda \rangle \bar{p}A)/(\langle N_\Lambda \rangle \bar{p}p) \approx \langle \nu_{\rm eff} \rangle$ and $R^A_{\bar{\Lambda}} = (\langle N_{\bar{\Lambda}} \rangle \bar{p}A)/(\langle N_{\bar{\Lambda}} \rangle \bar{p}p) \approx 1$, where $\langle \nu_{\rm eff} \rangle$ is the effective number of interactions in the nucleus.

(4) The experimental values of K^0 and Λ particle yields slightly exceed the similar value predicted by the FRITIOF-7.02 code, but their A dependences coincide within the error. We have $\sim (0.179 \pm 0.004) A^{(0.155 \pm 0.003)}$ for the K^0 mesons, and $\sim (0.054 \pm 0.003) A^{(0.202 \pm 0.007)}$ for the Λ hyperons.

There is a difference in yields of the $\bar{\Lambda}$ hyperons, where by FRITIOF-7.02 a growth of

$$\sim (0.060 \pm 0.002) A^{(0.074 \pm 0.004)}$$

is predicted.

Acknowledgements. We thank our colleagues in the RISC Collaboration for their contribution to all stages of the experiment. We are indebted to N.N. Roinishvili and J. Manjavidze for enlightening comments and stimulating discussions. This work was supported in part by the Academy of Sciences of the Republic Georgia (Grant no. 2.11).

References

1. M.Iu. Bogolyubsky et al., Yad. Fiz. **48**, 8733 (1988)
2. M.Iu. Bogolyubsky et al., Yad. Fiz. **43**, 1199 (1986)
3. M.Iu. Bogolyubsky et al., Yad. Fiz. **39**, 1436 (1984)
4. M.Iu. Bogolyubsky et al., Yad. Fiz. **50**, 683 (1989)
5. P.F. Ermolov et al., Report IHEP, Protvino 83-126 (1983)
6. B. Hanumajah et al., Nuovo Cim. A **68**, 161 (1982)
7. V.V. Anisovich et al., KFKI (1982) 36
8. U.P. Sukhatme et al., Phys. Rev. Lett. **45**, 5 (1980)
9. B. Nilsson-Almqvist, E. Stenlund, Comput. Phys. Commun. **43**, 387 (1987)
10. A. Javrichvili et al., Nucl. Instrum. Methods **177**, 381 (1980)
11. L.S. Vertogradov et al., Prib. Tekh. Eksp. **3**, 31 (1978)
12. E.M. Andreev et al., Report JINR, Dubna I3-8550 (1975)
13. S.P. Denisov, S.V. Donskov, Yu.P. Gorin et al., Nucl. Phys. B **61**, 62 (1973)
14. E.M. Andreev et al., Yad. Fiz. **35**, 700 (1982)
15. D.R. Ward et al., Phys. Lett. B **62**, 237 (1976)
16. H. Sumiyoshi et al., Report University Tokio,INS-Rep-460 (1982)
17. RISC collaboration., Report JINR, Dubna E1-83-449 (1983)
18. B.V. Batyunya et al., Report JINR, Dubna E1-82-475 (1982)
19. E.G. Boos et al., Report JINR, Dubna E1-83-449 (1983)
20. E.G. Boos et al., Z. Phys. C **26**, 43 (1984)
21. E.N. Kladnitskaya , Particles and Nuclei **13**, 669 (1982)